

# Experimental studies of kerosene injection into a model of a detonation chamber

Jan Kindracki \*

*Institute of Heat Engineering, Warsaw University of Technology  
21/25 Nowowiejska Street, 00-665 Warsaw, Poland*

## Abstract

The paper presents the results of experimental research of kerosene injection into the high speed nitrogen flow of a model of a detonation chamber. Kerosene was injected into the rectangular section of the model of the chamber, which had a width of 20mm. A plain orifice kerosene injector of various diameters was used. The injector was set perpendicular to the nitrogen flow. The nitrogen was injected through a slot of a certain size that created a choked flow.

Measurements of the nitrogen velocity distribution and numerical calculations for the chamber were performed in order to obtain data on the nitrogen speed inside the chamber. The nitrogen flow velocity in the experiments was in the order of 50–250 m/s, depending on the distance between the Prandtl probe and the inner wall. Measurements of the diameter of droplets injected into the model chamber were also taken. High-speed photography with a back light was utilized in the droplet diameter measurements. The values of the SMD, obtained for the stream of cold nitrogen (about 290 K), were of the order of 33–38  $\mu\text{m}$ . This provided information about the size of the droplets and their spatial distribution, which are key elements in the designing of the detonation chamber.

*Keywords:* kerosene injection, droplet distribution, SMD diameter, high speed photography

## 1. Introduction

The process of fuel injection into the chamber is one of the most important processes that take place in the combustion chamber. Optimal organization of this process enables the period of injection and mixing of fuel with air to be reduced, therefore reducing the dimensions and mass of the combustion chamber. The fuel injection process also has a strong impact on minimizing the amount of harmful gases emitted from the jet engine [1]. This is a very important issue

because jet engines typically operate mainly at high altitudes where the harmful components of exhaust gases may exist for a long time [2, 3].

Hamid and Atan [4] describe the studies of two commercial jet-swirl injectors. Commercially available injectors were tested in the studies. They produced two types of cone-shaped jet fuel spray: hollow and full in the middle. In the tests, the discharge coefficient and breakup length (the distance it takes the liquid film to disintegrate into droplets) were obtained as functions of the injection pressure. Liu and Reitz [5] describe a study into the mechanisms of droplets breaking in a fast stream of air flowing perpendicular to the direction of the fuel injection.

\*Corresponding author

*Email address:* jan.kindracki@itc.pw.edu.pl (Jan Kindracki )

Ordinary diesel fuel was used. In the tests, a specially designed piezo-electric drop generator was applied as an initiator. Air velocity in the experiments described was in the order of 68–331 m/s and the droplets generated were in the range of 69–198  $\mu\text{m}$ . Pictures of the process were taken with a resolution of 3  $\mu\text{m}$  by using a special microscope lens and with a single flash of 20 ns duration.

Wigley et al. [6] describe the study of high-quality gasoline injection (fuel pressure equal to 50–120 bar) into the ambient air conducted with Laser and Phase Doppler Anemometry (LDA/PDA). The measurements provided information about the average speed of the drops and their size. The Sauter mean diameter (SMD) value ranged from 20 to 80  $\mu\text{m}$ , depending on the case (injection pressure). The usefulness of the method used in the injection study was confirmed, but the method requires the droplets to be illuminated from the direction opposite to the camera lens, which can be problematic in some cases.

Doungthip et al. [7] describe a study on aviation Jet A and JP-8 fuel injection under supercritical conditions (with kerosene temperature above 400°C) with the use of a simple injection nozzle. The maximum injection pressure was relatively low: approximately 34.5 bar. A Schlieren system with a CCD camera was used to register the fuel injection. These studies were carried out in order to validate a numerical code. The main task of this code was to predict the angle and range of the fuel injected into the test chamber. Numerical studies of different models of injection and the formation of fuel-air mixture were described by Al-Omari [8]. These studies were aimed at checking the possibility of improving the quality of the mixture in an inlet duct. Various configurations of inlet duct, both curved and straight, for three different droplet sizes (30 m, 150 m, 180 m) were studied.

Another method of fuel injection was introduced by Zakrzewski et al. [9]. This work presents the results obtained from numerical calculations for supersonic liquid fuel injectors used in diesel engines and in ramjet engines. The paper shows the development of the computational schemes, based on commercial codes, which were then used to obtain the characteristics of the mixing of the liquid fuel with air in a situation where an oblique shock wave was present.

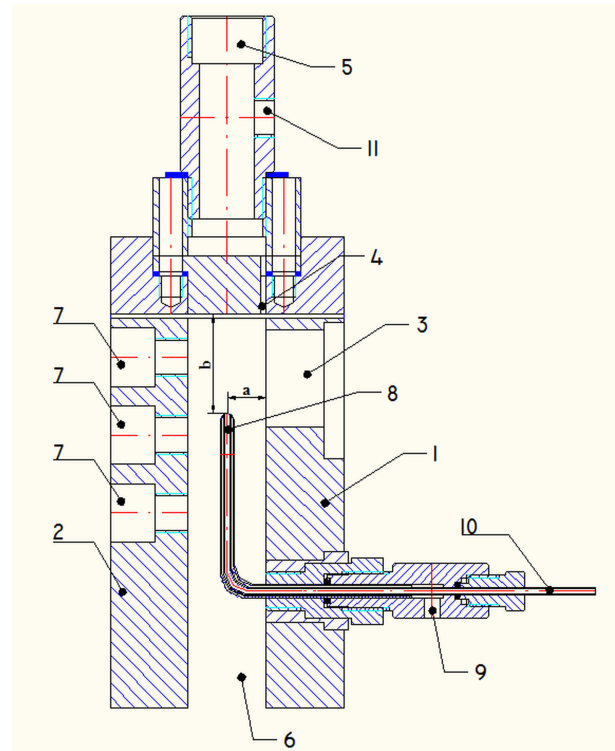
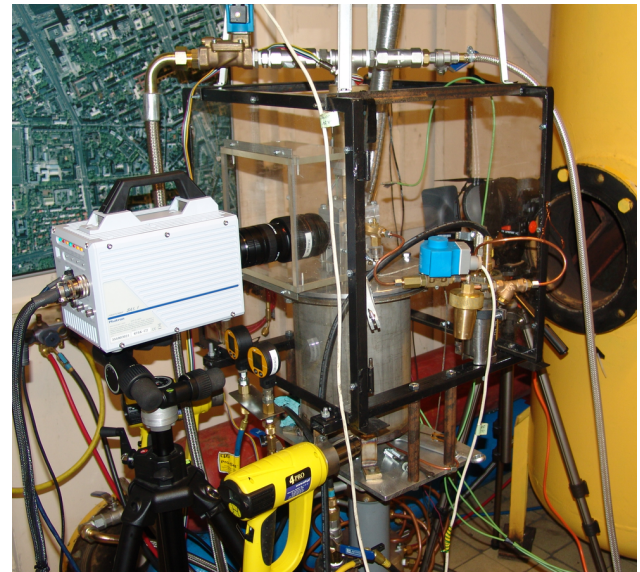
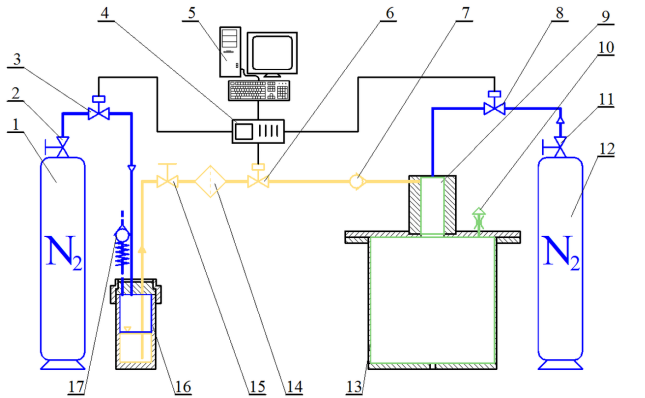


Figure 2: Experimental setup for nitrogen velocity measurement: 1—inner wall, 2—outer wall, 3—kerosene injector socket, 4—nitrogen injector, 5—nitrogen manifold, 6—outflow, 7—pressure transducers/thermocouple socket, 8—Prandtl probe, 9—static pressure gauge connector, 10—total pressure, gauge connector, 11—manifold static pressure transducers

## 2. The research setup

The experiments were conducted on a model detonation chamber. The term detonation chamber means an annular combustion chamber where thermal energy is released in the process of detonation. The use of a gaseous detonation process should lead to an increase in the thermal efficiency of the combustion process. More information on the design of and research into the detonation chamber can be found in the papers [10–12].

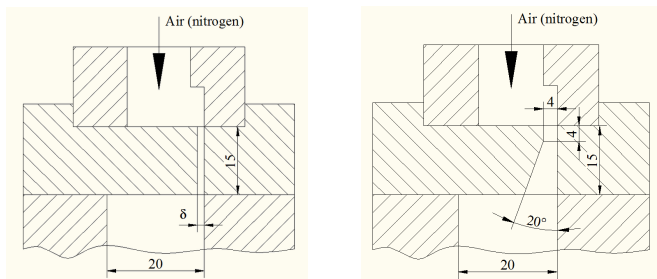
The test bench consisted of the model chamber, the fuel and nitrogen injection system, and the measurement system. The model chamber was connected to a special tank which received the combustible mixture



(a) schematic view: 1—bottle with nitrogen, 2—valve, 3—electromagnetic valve, 4—acquisition card, 5—computer, 6—electromagnetic valve, 7—one way direction valve, 8—electromagnetic valve, 9—research chamber, 10—silencer (outflow), 11—bottle valve, 12—bottle with nitrogen, 13—dump tank, 14—filters, 15—valve

(b) view of the stand

Figure 1: Research bench facility



(a) straight (nitrogen injector—case no. 1— $d = 2$  mm, nitrogen injector—case no. 2— $d = 4$  mm) (b) modified (nitrogen injector—case no. 3)

Figure 3: Design of nitrogen injector

formed inside the chamber and prevented it from igniting accidentally. A schematic diagram and a view of the test bench are presented in Fig. 1. The model chamber was constructed in the form of a rectangular channel closed on both sides by walls made of duralumin, simulating the inner and outer wall of the chamber (Fig. 2). Two plexiglas windows were mounted transversely to these walls to enable pictures to be taken of the injection process. The upper

part of the chamber was closed by the nitrogen injector. Three variants were constructed: two straight gaps with a width of 2 and 4 mm, and one complex gap of 4 mm in the shape of a simple conical nozzle. The nitrogen injector is shown in Fig. 3. The nitrogen at a specified pressure was supplied from a high pressure cylinder via supply lines, and a high-speed solenoid valve was used for flow rate control. The valve was controlled by using a data acquisition card and digital outputs. For safety reasons, nitrogen replaced air in the experiments involving the injection of kerosene. This significantly reduced the risk of accidental ignition of the kerosene vapour contained in the dump tank, whilst leaving the environmental conditions in the test chamber practically unaffected during the experiments.

The fuel supply system consisted of a tank with kerosene, two filters (250  $\mu\text{m}$ , 40  $\mu\text{m}$ ) and a direct acting solenoid valve. A pressure system with nitrogen as the working gas was used to pump the kerosene from the tank to the injector. The pressure supply system provided straightforward pressure control and an uncomplicated method for test-

Table 1: Parameters of the fuel injector used in the experiments

No	$d$ , mm	$l$ , mm	$L/d$ , mm	$\alpha$ , °	Scheme
1	0.4	2	5	0	
2	0.3	2	6.67	0	
3	0.2	2	10	0	
4	0.3	2.3	7.67	30	
5	0.3	2.3	7.67	-30	

ing at different pressures. Additionally, it enabled regulation of the mass flow rate of the fuel injected into the test chamber. The fuel injector was made of a simple hole of a certain diameter and length. The parameters and schemes of the injectors tested are listed in Table 1.

The measuring system consisted of two subsystems. The first subsystem included all temperature sensors and pressure sensors installed on the test bench: in the test chamber and in the nitrogen and fuel manifolds. The sensors were connected through amplifiers to the National Instruments USB 6259 measuring card. This card was also used to control the solenoid valves and high-speed camera. The second measurement subsystem consisted of a high-speed camera (Photron SA1.1 model 675K-C1) and a light source. The fuel droplet recordings were conducted using a shadowgraph method. This method involves registering the shadow of a droplet when the light source is set on the side opposite to the camera. A high-speed camera was required due to the parameters of the objects observed (drops): high movement speed of up to 80 m/s and small size, from teens to a few hundred micrometers, the high recording quality needed. In the experiments described, the typical frame rate was in the range 5,400–20,000 fps and single frame exposure time was 1  $\mu$ s. The need for the high speed of recording and the short time of exposure can be explained with the example of a 100  $\mu$ m diameter droplet moving with a velocity equal to 50 m/s. In the case the droplet will be moved by a half own diameter during the exposure time. The resolution of the images depends on the

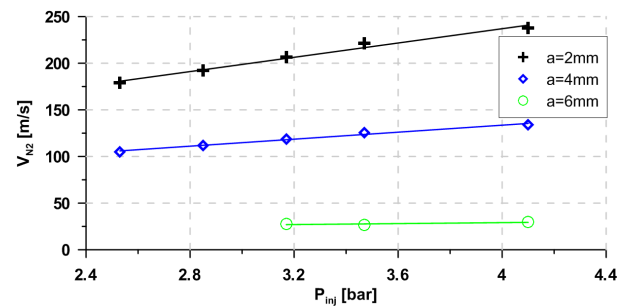


Figure 4: Nitrogen velocity ( $V$ ) measurements as a function nitrogen injection pressure ( $p$ ) and distance from the inner wall (see Fig. 2 dimension  $a$ —distance between the probe and a wall). Nitrogen injector—case no. 1

speed of the recording: 512×512 points for the highest and 1024×1024 for the smallest recorded rates. Such parameters required good lighting to illuminate the drops. A Nikon lens with a variable focal length (24–85 mm) and additional intermediate rings was used in the tests.

### 3. Measurements of nitrogen velocity

The first phase of the study focused on measuring the nitrogen velocity profile in the test chamber. For this purpose a Prandtl tube was mounted inside the chamber. To measure the differential pressure a PD-23 sensor (made by Keller) and static pressure sensor SEN-8700/2 (made by Kobold) were used. Additionally, in the location of the pressure gauge, measurements of static temperature were made with the use of a thermocouple and amplifier (both made by the

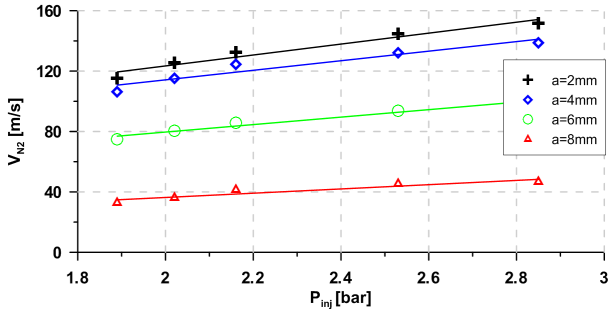


Figure 5: Nitrogen velocity ( $V$  measurements as a function of nitrogen injection pressure ( $p$ ) and distance from the inner wall (see Fig. 2 dimension  $a$ —distance between the probe and a wall). Nitrogen injector—case no. 2

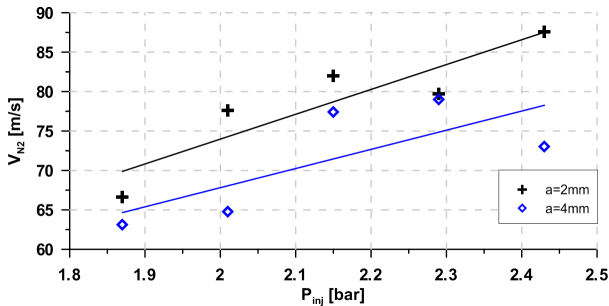


Figure 6: Nitrogen velocity ( $V$ ) measurements as a function of nitrogen injection pressure ( $p$ ) and distance from the inner wall (see Fig. 2 dimension  $a$ —distance between the probe and the wall). Nitrogen injector—case no. 3

Czaki Company). Measurements of these parameters made it possible to calculate the velocity of the nitrogen. The measurement was carried out at several distances from the inner wall of the channel, as shown in Fig. 4–Fig. 6.

A two-dimensional numerical calculation of the process was carried out in order to obtain more data concerning the process. The commercial program Fluent 6.3 was used for the calculation. In the program, the ideal gas model and the  $k$ - $\epsilon$  with RNG turbulence model were applied. The results of the calculations of the nitrogen injection pressure at 4 bar are shown in Fig. 7. The figure shows the nitrogen velocity as a function of the sensor position and nitrogen injection pressure. The measurement was carried out at a distance of 25 mm from the nitrogen injector.

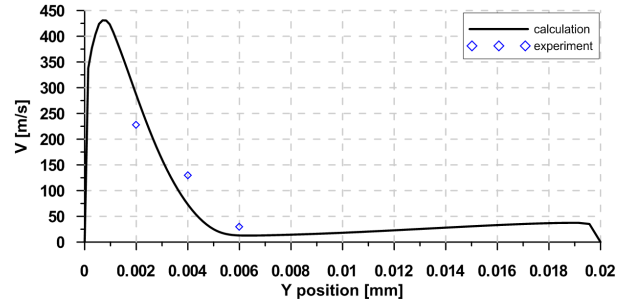


Figure 7: Velocity  $b = 25$  mm from the nitrogen injector ( $p = 4$  bar, numerical calculations). Y position—distance between the numerical probe and the inner wall (with fuel injector)

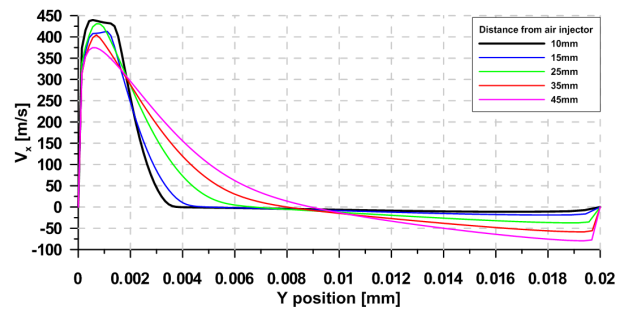


Figure 8: Velocity component ( $V$ ) in Y-direction along the width of the channel for different distances from the nitrogen injector ( $p = 4$  bar, numerical calculations)

Nitrogen flow calculations were carried out in a stationary flow because an interesting issue in this case was the steady-state operation of kerosene injectors and the fixed flow in the nitrogen injector. The filming of the droplet injection process began when the injection started and continued until quasi steady flows of both components were obtained (the time of the tests included both transient and steady flow). Analysis of droplet size during this process allowed the tracking of changes in droplet diameter during the transient flow. However, to compare the different injectors, droplet diameter distribution was used for the steady flows. Therefore, numerical calculations for the steady flow were carried out.

A comparison of Fig. 4 and Fig. 7 demonstrates clearly that the calculated results are comparable with those obtained experimentally, especially in that the accuracy of the probe set used in the experiments was 0.5 mm. These results confirm that the design of the chamber results in a narrow jet of fast

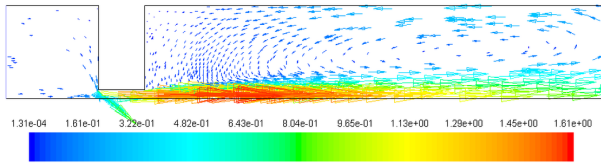


Figure 9: Velocity vectors from numerical calculations  $p = 4$  bar. (left side—injection of the nitrogen inflow, right side—outflow)

moving nitrogen near the inner wall of the chamber. The injected nitrogen velocity values change very rapidly, even at a minimal distance from the inner wall. Moreover, at some distance from the inner wall there is a negative value of the longitudinal component of the nitrogen velocity ( $V$  component, see Fig. 8), which proves the existence of a reverse flow (vortex), located at the outer wall of the chamber, as shown in Fig. 9. The existence of the vortex in the corner of the chamber was confirmed by the pictures of the process of kerosene injection. The sequence of pictures presented in Fig. 10 shows the movement of kerosene droplets in the opposite direction to the main nitrogen stream. This swirling nitrogen flow is widely used in combustion chambers. It enables a better mixing of the fuel with the oxidizer and helps create a more homogeneous mixture.

The location of the fuel injection on the inner wall of the detonation chamber has several advantages. The narrow fast moving nitrogen jet has a kinetic energy comparable with relatively slow kerosene injection (the density difference was of the order of hundreds of times.) Thanks to this, the fuel jet starts to break just at the exit of the injector. As a result of this process, relatively small fuel droplets were obtained at distances of the order of several millimeters from the injector, which was confirmed by measurements presented in Section 4.

#### 4. Measurement of kerosene injection

One of the most important parameters measured during studies on fuel injection into a combustion chamber is the size of the fuel droplets. Droplet size has a significant impact on the time of the generation of a high, quality, fuel-oxidizer mixture. A proper injector ensures the adequate size and required spatial

distribution of the droplets in the combustion chamber. For the evaluation of the quality of the injection, the Sauter mean diameter (SMD) is usually chosen. In order to determine this diameter a large collection of experimental data needs to be prepared. In the experiments described, these data were obtained using the shadow picture method described above. The diameter of the droplet was obtained basing on the registered picture with use of the CAD package. The geometrical scale of the picture was determined using registration of an object of known size.

Unfortunately the technique also has some drawbacks. One of them is that during the observation of a small area we can clearly only see those droplets which are in the plane of focus of the optical system. It is impossible to obtain information about the diameter of droplets over the entire volume of the test chamber. This problem can be solved partly by performing further experiments with the same injection parameters, and by changing the plane of focus. After several experiments, a three-dimensional distribution of droplets in the combustion chamber can be obtained. However, it is laborious and time consuming.

Fig. 11 shows the successive sequence of the kerosene injection process for the fuel injector of 0.2 mm in diameter (first 3 pictures show unsteady phase of the process and the last one presents the steady phase). The injector was placed perpendicular to the chamber wall. The first frame shows the beginning of fuel injection, when the nitrogen flow has only just begun. The fuel injection pressure in this case was equal to 19 bar. It is clear that the fuel jet breaks down into smaller parts, but still reaches the opposite wall (in the pictures 75% of the width of the channel is visible.) The next two frames show the growth of nitrogen flow and the increasing fragmentation of the jet of kerosene. The last frame shows a stabilized flow of nitrogen and kerosene. The smaller droplets are visible in the high-speed flow (right hand side of the picture,) and the larger droplets in the outer part of the chamber (left hand side of the picture.) Furthermore, comparison of successive frames shows pulsations in the jet of kerosene. The pulsations allow the better filling of the entire width of the channel by the fuel droplets. In addition, the location of nitrogen injection causes a back-flow near

the outer wall of the channel. This vortex transports part of the fuel (see Fig. 10—large drops on the left side of the photo) upstream, and this result with even better mixing of the fuel with the nitrogen. The droplet size distribution in this test (no. 1) is shown in Fig. 13a. Most of the droplets have diameters in the range of 20–40  $\mu\text{m}$ , and the SMD calculated was about 33–38  $\mu\text{m}$ . It should be noted that these studies were carried out at ambient temperature. It is assumed that an increase in nitrogen temperature would reduce the size of the droplets, but their measurement by the method described above is presently impossible in this research facility.

The other test (no. 2) for the fuel injector of 0.3 mm in diameter and inclined at 30 degrees upstream is shown in Fig. 12. The fuel jet shown in the first frame (minimal flow of nitrogen) reaches the wall and reflects. As the nitrogen flow rises, the fuel flow range continuously decreases. After reaching the nominal value of the nitrogen's mass flow rate, the fuel jet bends just behind the outlet of the injector. Comparing the final picture with the final picture from test no. 1, it shows a much smaller filling of the chamber by the fuel droplets (especially near the outer wall, left hand side.) The graph presented in Fig. 13b shows that in this case the SMD value was almost doubled in comparison with the previous one, and equal to 63–67  $\mu\text{m}$ .

Such a difference in the size of the droplets in the cases under consideration might be explained by the different nitrogen injectors used. In test no. 1, the nitrogen was injected through a narrow, 2 mm width slot. As a result, a narrow jet of nitrogen flowing near the inner wall of the chamber was achieved. This is confirmed by measurements of the velocity (see Fig. 4.) At a distance of 6 mm from the wall, the flow velocity decreased to about 30 m/s, while near the wall (2 mm), it is about 200 m/s. Such rapid changes in velocity meant that the fuel jet was effectively broken up by the transverse nitrogen stream. The large aerodynamic forces created caused the breaking up of the fuel stream into small droplets. In test no. 2, the nitrogen injection was carried out through a slit with a width of 4 mm, extended at an angle of 20 degrees, which created a kind of simple flat nozzle. This resulted in the rapid expansion of the nitrogen flow (see Fig. 6) and a reduction in the aero-

dynamic effects on the fuel-oxidizer boundary, and thus increased droplet size. But, the greatest impact on droplet size in these two reported cases was observed for a change of orifice diameter from 0.2 to 0.3 mm

## 5. Summary and conclusions

The study described was aimed at verifying the correctness of the design concept of the injection of liquid kerosene into the nitrogen flow (nitrogen in these experiments, but air in real life) in a detonation chamber. Nitrogen velocity distributions in the chamber were studied for three injector geometries. The size of the injected droplets was also measured in the research. The results confirmed that the oxidizer injector will result in a narrow nitrogen flow moving along the inner wall of the chamber. The formation of the reverse flow was an additional effect of this kind of nitrogen injection. The reverse flow helps in the further defragmentation of fuel droplets and results in a more uniform distribution of droplets in the chamber.

The droplet size measurements, carried out with use of the shadowgraph method, confirmed the usefulness of this method for this type of injection test. It was also found that high quality equipment was required to obtain correct results. The obtained value of the SMD of the order of 33–38  $\mu\text{m}$  for the stream of cold nitrogen (about 290 K) suggests that these droplets quickly evaporate and form a combustible mixture. Additional heating of the air (in the real engine) should accelerate this effect. This confirms the correctness of the design assumptions for the fuel and nitrogen (air) injectors. The simplicity of the jet fuel injector can also help reduce the costs of enforcement. It also provides the possibility of spacing optimization in order to obtain a more uniform composition of the mixture around the perimeter of the chamber.

### *Acknowledgements*

This work was supported by the Ministry of Science and Higher Education, Republic of Poland, project no. 838/B/T02/2009/37. The author would like to thank engineering diploma student Szymon Fulara for his help in conducting the experiments.

## References

- [1] A. Tudosi, *Aeronautics and Astronautics*, InTech, 2011, Ch. Aircraft gas-turbine engine's control based on the fuel injection control, pp. 305–330.
- [2] H. Johnston, D. Kinnison, D. Wuebbles, Nitrogen oxides from high-altitude aircraft: An update of potential effects on ozone, *Journal of Geophysical Research* 94 (D13) (1989) 16351–16363.
- [3] U. Schumann, The impact of nitrogen oxides emissions from aircraft upon the atmosphere at flight altitudes—results from the aeronox project, *Atmospheric Environment* 31 (12) (1997) 1723–1733.
- [4] A. Hamid, R. Atan, Spray characteristics of jet–swirl nozzles for thrust chamber injector, *Aerospace Science and Technology* 13 (2009) 192–196.
- [5] Z. Liu, R. Reitz, An analysis of the distortion and breakup mechanisms of high speed liquid drops, *International Journal of Multiphase Flow* 23 (1997) 631–650.
- [6] G. Wigley, J. Heath, G. Pitcher, W. A., Experimental analysis of the response of a laser/phase doppler anemometer system to a partially atomized spray, *Particle & Particle Systems Characterization* 18 (2001) 169–178.
- [7] T. Dounghthip, J. Ervin, T. Williams, B. J., Studies of injection of jet fuel at supercritical conditions, *Industrial & Engineering Chemistry Research* 41 (2002) 5856–5866.
- [8] S. Al-Omari, Numerical simulation of liquid fuel sprays evolution and the subsequent vapor/air-mixture formation in a duct with a 90-bend, *International Communications in Heat and Mass Transfer* 35 (2008) 197–203.
- [9] S. Zakrzewski, B. Milton, K. Pianthong, M. Behnia, Supersonic liquid fuel jets injected into quiescent air, *International Journal of Heat and Fluid Flow* 25 (2004) 833–840.
- [10] P. Wolanski, J. Kindracki, T. Fujiwara, *Pulsed and Continuous Detonations*, Torus Press, Moscow, 2006, Ch. An experimental study of small rotating detonation engine, pp. 332–338.
- [11] J. Kindracki, P. Wolanski, Z. Gut, Experimental research on the rotating detonation in gaseous fuels-oxygen mixtures, *Shock Waves* 21 (2011) 75–84.
- [12] J. Kindracki, A. Kobiera, P. Wolański, Z. Gut, M. Foliński, K. Łświdzki, *Advances in Propulsion Physics*, Torus Press, 2011, Ch. Experimental and Numerical Research on the Rotating Detonation Engine in Hydrogen-air Mixtures.

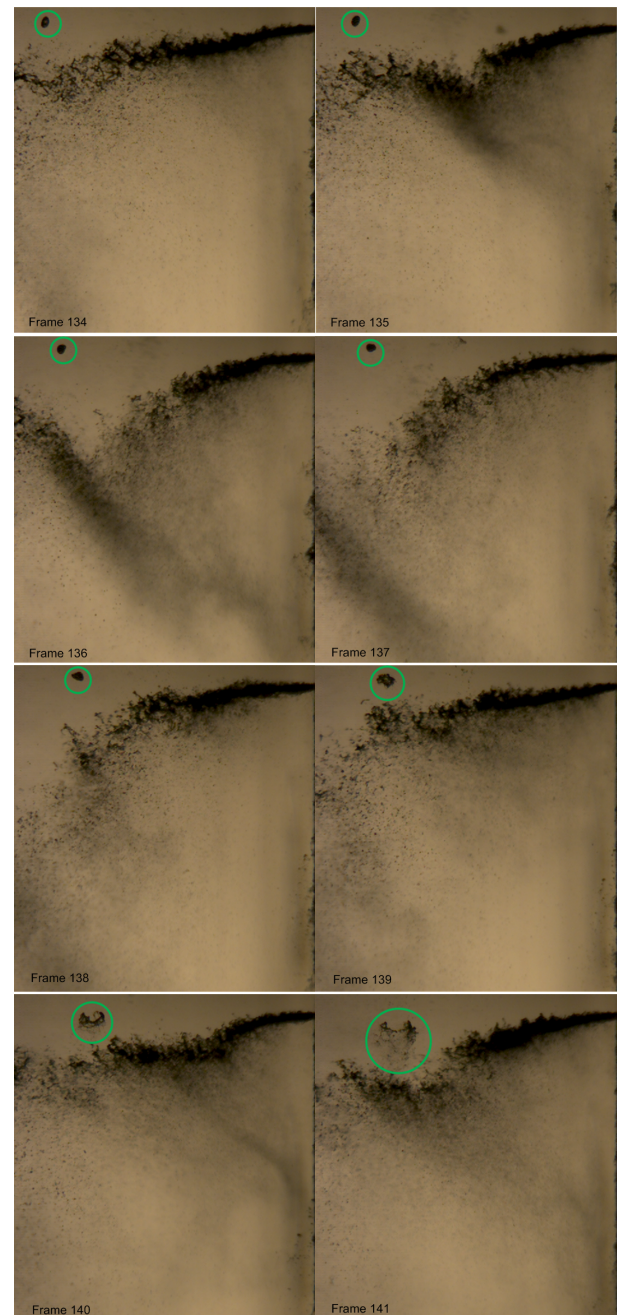
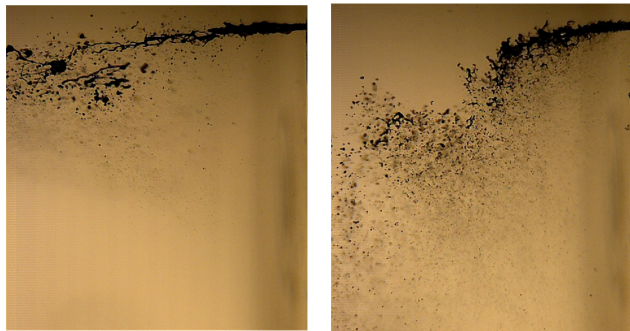


Figure 10: Injection sequence showing the droplet moving upstream (green circle upper left corner) transporting it to the core flow where it is broken into smaller parts (time resolution between pictures is 50  $\mu$ s)





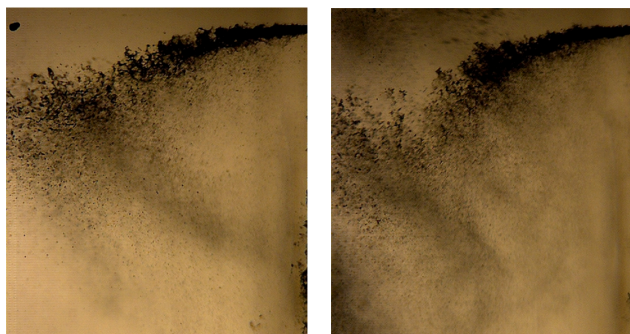
(a) just after start of injection of kerosene without nitrogen flow—1.15 ms

(b) 4.5 ms



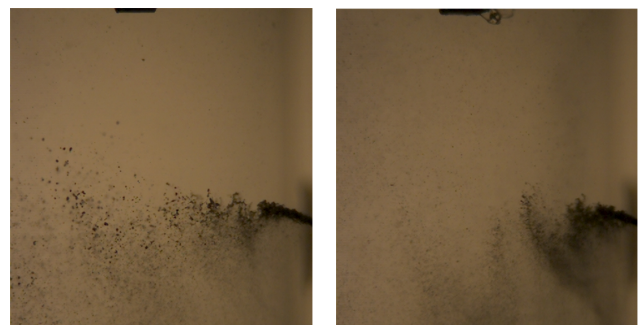
(a) just after start of injection of kerosene without nitrogen flow—8.55 ms

(b) 10.5 ms



(c) 6.2 ms

(d) 7.15 ms (steady flow)

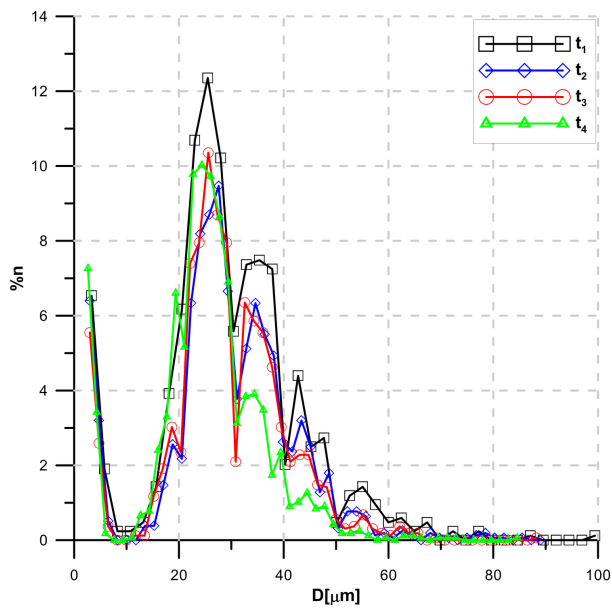


(c) 12.5 ms

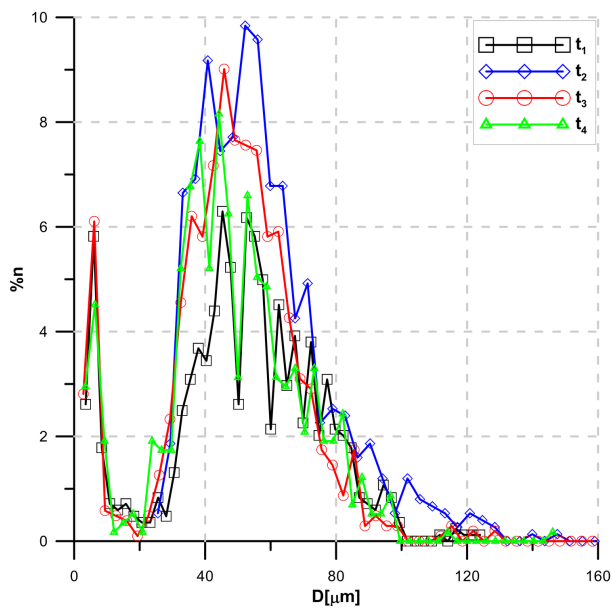
(d) 15 ms (steady flow)

Figure 11: Sequence of the injection process for the 0.2 mm diameter injector, perpendicular to the nitrogen flow from the injector with nitrogen slot no. 3 (slot width 4 mm with an angle of 20 deg, 20,000 fps, exposure time 1  $\mu$ s) test no. 1

Figure 12: Sequence of the injection process for 0.3 mm diameter injector, upstream (30 deg) to the nitrogen flow from the injector with nitrogen slot no. 1 (slot width 2 mm, 20,000 fps, exposure time 1  $\mu$ s) test no. 2



(a) test no. 1  $D_{32} = 40.66 \mu\text{m}(t_1)$ ,  $D_{32} = 38.81 \mu\text{m}(t_2)$ ,  
 $D_{32} = 36.69 \mu\text{m}(t_3)$ ,  $D_{32} = 33.28 \mu\text{m}(t_4)$



(b) test no. 2  $D_{32} = 67.89 \mu\text{m}(t_1)$ ,  $D_{32} = 75.81 \mu\text{m}(t_2)$ ,  
 $D_{32} = 63.65 \mu\text{m}(t_3)$ ,  $D_{32} = 63.9 \mu\text{m}(t_4)$

Figure 13: Percentage distribution of droplet size as a function of droplet diameter (statistics calculated on the basis of data collection from 580 to 1670 drops)